ZCZVT INVERTERS WITH MAGNETICALLY COUPLED AUXILIARY POLE

Mário L. S. Martins[1], Carlos M. O. Stein[1], Jumar L. Russi[2], José R. Pinheiro[3], Hélio L. Hey[3]

[1]PROCEN – GEPEP, Universidade Tecnológica Federal do Paraná - UTFPR
CEP 85503-390 Pato Branco, PR, BRASIL
mlucio@utfpr.edu.br, cmstein@utfpr.edu.br

[2]Universidade Federal do Pampa - UNIPAMPA
CEP 97546-550 Alegrete, RS, BRASIL
jrussi@ gmail.com

[3]GEPOC, Universidade Federal de Santa Maria - UFSM
CEP 97105-900 Santa Maria, RS, BRASIL
hey@ctlab.ufsm.br, renes@ctlab.ufsm.br

***Abstract* – Existing Zero-Current Transition and Zero-Current Zero-Voltage Transition inverters provides favorable switching conditions for IGBT semiconductors increasing significantly the reactive energy of the converter. This situation off-set the benefits accomplished by abovementioned soft-switching techniques. This paper presents a novel family of Zero-Current Zero-Voltage Transition inverters that overcome this problem by using no resonant tank in the auxiliary circuit. It accomplishes the favorable soft-switching conditions with a magnetically coupled auxiliary voltage source which is derived directly from the inverter filter inductor. Theoretical analysis of the inverter operation is presented and it is verified experimentally from a 1kW, 40kHz, laboratory prototype. The obtained experimental results prove the reliability of the proposed family of ZCZVT inverters.**

***Keywords* - Inverter, Soft-switching, Zero-Current Transition, Zero-Voltage Transition.**

I. INTRODUCTION

The rise of switching frequency in industrial power inverters provide significant reduction of physical size, weight and cost of reactive elements, as well as electrical performance enhancements [1]. To achieve such characteristics it is required fast semiconductor devices with low switching losses. As semiconductor technologies had improved through the years, the MOS-bipolar transistor such as the Insulated Gate Bipolar Transistor (IGBT) has becoming predominant in many industrial applications. The IGBT is a result of the combination of MOS and bipolar structures in the same device [2], yielding a voltage-driven device with low on state losses, low switching losses and a high current capability.

Despite of continuous technological improvements, the IGBT still far from the ideal switch characteristics. After a number of generations the IGBT still presents a trade off between on state voltage drop and turn-off switching time, that constrain its total power handling capability [3]. In order to alleviate the IGBT switching losses and thus, lessen the aforementioned trade off, soft-switching techniques, constantly discussed in the past decades, seem to be an attractive alternative [4].

Due to the IGBT turn-off switching limitations, the Zero-Current Transition (ZCT) [5,6] and Zero-Current Zero-Voltage Transition (ZCZVT) [7,8] techniques appear as the most adequate approaches. The ZCT technique eliminates the current and voltage overlapping completely during the turn-off process, providing favorable conditions for a minority carrier type device to be turn-off. In the ZCT inverters the reverse recovery of diodes also can be reduced, nevertheless, voltage transitions across the semiconductors are quite like hard-switching devices. The ZCZVT technique combines Zero-Current switching turn-off conditions and Zero-Voltage switching turn-on conditions for the same device, reducing IGBT losses and improving EMI performance. Nevertheless, the price paid for such favorable switching conditions is the addition of a resonant auxiliary circuit that yields in additional reactive energy [9]. This energy is handled by the auxiliary devices which result in additional conduction and switching losses. To effectively improve the inverter efficiency it is necessary that additional losses in the auxiliary circuit to be smaller than the saved main devices switching losses. The auxiliary circuit for ZCT and ZCZVT inverters presented hitherto relay on the operation of a resonant LC tank that produces a huge amount of reactive energy that may offset the inverter efficiency gain. This situation reduces the advantages of using soft-switching techniques such as ZCT and ZCZVT.

In order to contribute to the development of the ZCZVT technique, this paper presents a novel family of ZCZVT inverters with lower reactive energy. To achieve such advantage the resonant tank is replaced by a magnetically implemented auxiliary voltage source that provides the necessary energy to magnetize auxiliary inductor every time a main switch commutation takes place. The named *ZCZVT inverters with magnetically coupled auxiliary pole* produce a linear like current with small resonant intervals that ensures limited *dv/dt* and losses.

This paper is organized as follows. Section II introduces a generalized concept for resonant transition converters based on the Auxiliary Source Concept applied to a hypothetical

Manuscript received on 15/05/2008. Revised on 19/10/2009. Accepted for publication on 17/01/2010 by recommendation of the Editors of the Special Section on Efficient Use of Energy João Carlos Fagundes and Felix Alberto Farret.

Resonant Transition PWM inverter. Section III describes a synthesis methodology for the resonant transition inverters. In Section IV, a Class of magnetically-coupled auxiliary pole ZCZVT inverters is presented and analyzed. Section V presents the experimental results. Finally, Section VI presents the conclusions from the analysis and the experimental results.

II. A GENERALIZED CONCEPT FOR RESONANT TRANSITION CONVERTERS

A generalized concept concerning the Resonant Transition technique can be defined assuming that any Resonant Transition inverter presented in the literature can be represented by the simplified circuit diagram, as shown in Figure 1. A hypothetical Resonant Transition PWM inverter is a network M for which assumptions A1 through A4 is satisfied:

Assumption A1: *"Any Resonant Transition Inverter provides an alternative low impedance path to the load current during one or both commutation processes of the PWM pole"*.

Assumption A2: *"The auxiliary low impedance path is a network N that consists of only the following elements:*

1. *An ideal current source (I) that plays the role of the inverter load current;*

2. *A dependent voltage source (v_{xy}) that represent the voltage across the load. The voltage vxy is dependent on the switching function applied to the PWM pole. In other words it is a function of the inverter modulation. To simplify the analysis it is defined for only one switching period instead of the whole modulation period as,*

$$v_{xy} = V_{zy}\left[1-\mu\left(t-t_1\right)+\mu\left(t-t_5\right)\right] \qquad (1)$$

3. *A dependent voltage source vaux that plays the role of the Auxiliary Voltage Source (AVS).*

4. *At least one commutation inductor that directly absorbs or delivers energy (current buffer) to the PWM basic building block ensuring Zero-Voltage and or Zero-Current switching for the main semiconductors of the pole"*.

Assumption A3: *"The power flow through the commutation inductor is achieved by means of the control of vaux. The control variable (i_{CV} or v_{CV}) for v_{aux} depends on a set of elements that can comprises switches, transformers, inductors, coupled-inductors, capacitors, resistors, independent current and voltage sources"*.

Aiming to simplify the future analysis, vaux is assumed to be a voltage-controlled voltage source (Figure 2), as well as the proportionality constant μ that relates the voltage across its terminals is assumed to be unit. Thus, $v_{aux} = \mu v_{cv}$ becomes, $v_{aux} = v_{cv}$.

Assumption A4: *"The dependent voltage source v_{aux} (or its control variable v_{cv}) can be presented as a Class A AVS; as a Class B AVS; or a Class C AVS.*

From the generalized concept concerning the Resonant Transition technique described above, the associations of the switching techniques (ZCT, ZVT and ZCZVT) with the conceptual definitions (Function, Class and Form) are given in Table I.

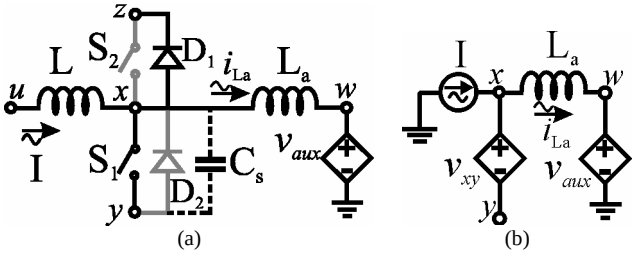

Fig. 1. Basic Resonant Transition PWM Block. (a) With PWM switch realization; (b) With dependent voltage sources simplification.

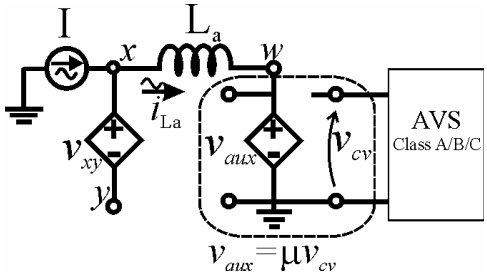

Fig. 2. Basic Resonant Transition PWM Block with a Voltage-controlled voltage source v_{aux} realization.

It can be seen that the concept of AVS classes based on [10] is assessed. The Function (or math function) provides a broader concept; meanwhile the *Class* and *Form* concepts are closer to the actual circuit behavior and thus, provide more insight to the circuit structure and functionality.

A. The AVS circuit structure and operation principle

There are only two basic mathematical functions that can fully represent the resonant transition mechanism, a *continuous (co-)sinusoidal time varying function* and a *discontinuous step function*. These functions produce the two essential classes of Auxiliary Voltage Source (AVS), named *Class A*, that are characterized by a *step waveform*; and *Class C*, that is characterized by a *(co-) sinusoidal waveform*. It can be seen by inspection of Figure 3 that a third Class, named *Class B* can provide an AVS to assist only the first v_{xy} transition, which means that it can only be used for produce ZVT inverters. The AVS theoretical waveforms are plotted in Figure 4.

Differently from the DC-DC or single-phase PFC converters, where a current unidirectional auxiliary circuit is used and the concept of the AVS Classes is sufficient to

TABLE I
Generalized Resonant Transition Concept and relationship.

Math functions	AVS Class (v_{aux})	Form of AVS (v_{aux})	Family of Soft-switching	
Discontinuous stepped	A	Stepped waveform	ZVT **ZCT**	**ZCZVT**
	B	Constant waveform	ZVT	---
Continuous time varying	C	Co-Sinusoidal waveform	ZVT	ZCZVT

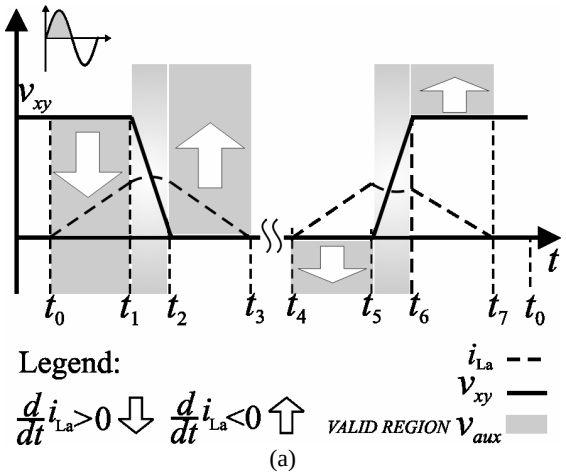

Fig. 3. Region of valid values for the v_{aux} function, according to the waveforms of v_{xy}, i_{La}. (a) Positive load semi-cycle; (b) Negative load semi-cycle.

reproduce the actual circuit behavior of the circuits, the current bi-directional auxiliary circuits employed by the Resonant Transition Inverters are more complex, as described below.

1) Co-sinusoidal function based AVS (Class C) - The structure of the Class C AVS presents can be grouped in two parts, the "*reactive elements*" and the "*excitation source*" (v_{exc}). These "*reactive elements*" are basically inductances and capacitances (resonant tank L_r-C_r) that store energy to commutate the main PWM pole. In some ZVT circuits, voltage clamps are employed to limit the resonant capacitor

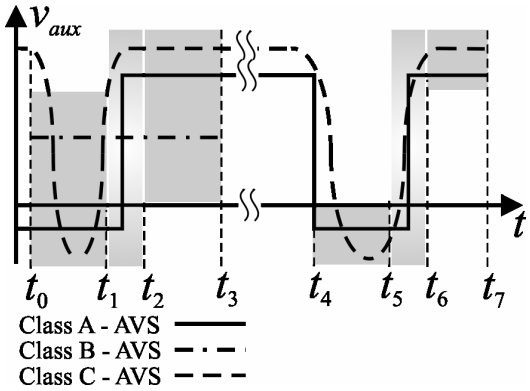

Fig. 4. Basic AVS waveforms for classes A, B and C considering a positive load current, according to Fig. 3(a).

energy (Figure 5(a)) [11]. The v_{exc} is comprised by a set of constant voltage sources (V_{Ap}, V_{An}) and the auxiliary pole S_{a1}-S_{a2}. This pole can be realized with two active [5] devices or with an active and one passive switch [12]. Switches S_{a1} and S_{a2} operate in such way that the voltage at the terminal '*t*' can change its value and so, the resonance provided by the resonant tank L_r-C_r can vary its characteristics. This active v_{exc} is explored by ZCT inverters in order to improve switching conditions for the some [13] or all [5] semiconductor devices. Alternatively to the active v_{exc} where the switches S_{a1}-S_{a2} commutate during the auxiliary circuit operation, the passive v_{exc} is used just to trigger the auxiliary circuit. In this approach, generally used in ZVT topologies [11], the state of the switches S_{a1} and/or S_{a2} is held until the end of the PWM pole commutation process. It must be highlighted that, despite of a passive or active "*excitation source*" be implemented, the main characteristic of the *continuous (co-)sinusoidal time varying function* AVS (Figure. 5(a)) is that no discontinuity in the (co-)sinusoidal voltage (v_{cv}) is presented.

2) Discontinuous Step based AVS (Class A) - For the discontinuous step function AVS the "*reactive elements*" are no longer necessary. Although, the v_{exc} present a more complex set of voltage sources, its association with a *full-controlled auxiliary pole* (Figure 5(b)) or two *semi-controlled auxiliary poles* (Figure 5(c)) directly handles the voltage across the commutation inductor. For the v_{exc} implemented with two semi-controlled auxiliary poles there is an individual set of constant voltage sources (V_{a1p}, V_{a2p} and V_{a3p}) for the positive-cycle of the load and another (V_{a1n}, V_{a2n} and V_{a3n}) for the negative-cycle of the load. The

TABLE II
Symmetric configurations and restrictions for the auxiliary voltage sources.

Config.	Auxiliary Voltage Sources			$I>0$ and S_{a1}/D_{a2}		$I<0$ and S_{a2}/D_{a1}	
	V_{a1}	V_{a2}	V_{a3}	$v_{xy}=0$	$v_{xy}=V_{zy}$	$v_{xy}=0$	$v_{xy}=V_{zy}$
1	$\neq 0$	$=0$	$=0$	$V_{a1}>0$	$V_{a1}>-V_{zy}$	$-V_{a1}>0$	$-V_{a1}>-V_{zy}$
				$V_{a1}<V_A$	$V_{a1}<V_A-V_{zy}$	$-V_{a1}<V_A$	$-V_{a1}<V_A-V_{zy}$
2	$=0$	$\neq 0$	$\neq 0$	$V_{a2}>0$	$V_{a2}>-V_{zy}$	$-V_{a2}>0$	$-V_{a2}>-V_{zy}$
				$V_{a3}<V_A$	$V_{a3}<V_A-V_{zy}$	$-V_{a3}<V_A$	$-V_{a3}<V_A-V_{zy}$
3	$\neq 0$	$\neq 0$	$\neq 0$	$V_{a1}+V_{a2}>0$	$V_{a1}+V_{a2}>-V_{zy}$	$-(V_{a1}+V_{a2})>0$	$-(V_{a1}+V_{a2})>-V_{zy}$
				$V_{a1}+V_{a3}<V_A$	$V_{a1}+V_{a3}>V_A-V_{zy}$	$-(V_{a1}+V_{a3})<V_A$	$-(V_{a1}+V_{a3})<V_A-V_{zy}$

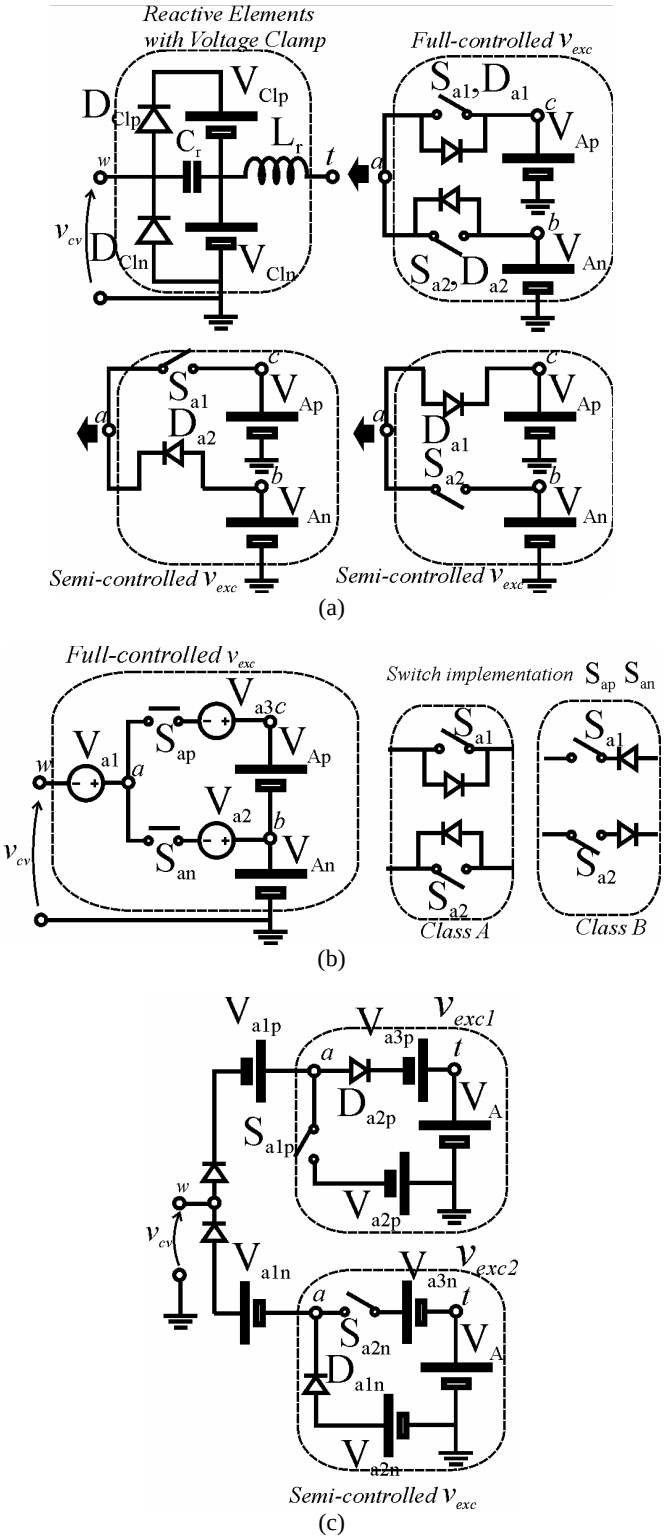

Fig. 5. Circuit diagrams for the AVS Classes. (a) Class C; (b) Class A with full-controlled "excitation source" and Class B; (c) Class A with semi-controlled "excitation source".

restrictions that ensure the right operation of the *Class A* AVS are derived in [14,15] for the six possible configurations of the *Class A* AVS. Table II shows the three symmetric configurations, as well as the restrictions for the corresponding voltage sources (V_{a1}, V_{a2} and V_{a3}). Assuming positive-cycle of the load, only one of the constant voltage sources (V_{a1p} or V_{a2p}) is required to the proper operation of the circuit. In the same way, the negative-cycle of the load only (V_{a1n} or V_{a2n}) is required. Nevertheless, the combination of the three voltage sources provides a family of topologies (as shown in Table II). As one can see, the polarities of the voltage sources (V_{a1p}, V_{a2p} and V_{a3p}) is exactly opposed to the polarities of the voltage sources (V_{a1n}, V_{a2n} and V_{a3n}), this implies that bi-directional voltage sources (V_{a1}, V_{a2} and V_{a3}) with stepped functions can be used to simplify the *Class A* AVS as shown in Figure 5(b). The restrictions for the symmetric configurations of the *Class A* AVS are shown in Table II and are valid for both "*excitation source*" implementations.

3) Discontinuous Step based AVS (Class B) - The *Class B* is characterized by a *constant waveform* obtained from a DC voltage source. Therefore, making use of a passive v_{exc} and an arrangement of constant voltage sources as those shown in Figure 5(c) without (V_{a1}, V_{a2} and V_{a3}), a *Class B* AVS can be obtained. Hence, the *Class B* AVS can be seen as a particular case of the *Class A*, where a passive v_{exc} is used.

This Section discloses that the relevance of the "*excitation source*" concept for the Resonant Transition inverters and also demonstrates that considerable improvements in the AVS implementations are achieved enhancing the "*excitation source*" characteristics.

It becomes clear that depending on the "*excitation source*" action, the same circuit structure for an AVS can provide different Classes and Resonant Transition techniques. For instance, *Class C* ZVT and ZCT shares the same circuit structure, nevertheless the ZCT active "*excitation source*" and the ZVT passive "excitation source" drive these techniques to different characteristics. On the other hand, a *Class A* ZVT or ZCZVT inverter employ an active "excitation source" that is very similar to the circuit structure of the *Class B* ZVT with passive "*excitation source*".

III. SYNTHESIS OF GENERALIZED RESONANT TRANSITION INVERTERS

According to Table I the ZCT Resonant Transition converters family make use of a *continuous time varying (co) sinusoidal function* to establish the resonant transition mechanism, which is classified as a *Class C* auxiliary voltage source (AVS) or v_{aux}. The *Class C* AVS is capable by itself to provide the charging and discharging polarity to inductor L_a, nevertheless it also uses a full-controlled excitation source (v_{exc}) that also can provide the charging and discharging polarity to L_a. It results in an extra degree of freedom that is used for producing different converter switching strategies. Nonetheless the price paid for such redundancy is a higher reactive energy that increases conduction losses.

By Table I it is clear that there is an opportunity to explore the *discontinuous step function* to establish the resonant transition mechanism in ZCT and ZCZVT converters (shaded cells).

The main advantages of using the so called *Class A* AVS is two fold, the first one is avoid the reactive energy associated to the resonant process that characterize the *Class*

C AVS; the second is to make the conduction losses of the auxiliary circuit to be proportional to the load current.

The challenge to implement the *Class A* AVS to ZCT and ZCZVT inverters is to obtain the required voltage sources ($V_{a1p,n}$, $V_{a2p,n}$, and $V_{a3p,n}$) for the two semi-controlled "*excitation source*" implementation or (V_{a1}, V_{a2}, and V_{a3}) for the full-controlled "*excitation source*" implementation.

A. Auxiliary Voltage Sources Implementation

The utilization of magnetic elements to perform the auxiliary voltage sources (V_{a1}, V_{a2} and V_{a3}) allows the inversion of polarity necessary to implement the full-controlled "*excitation source*" ensuring simplicity, ruggedness and compactness to the auxiliary circuit. The magnetic realization of V_{a1}, V_{a2} and V_{a3} consist on the use of a single magnetic core with a primary winding forming a closed loop with a voltage source and one or more secondary winding(s) that play(s) the role of each auxiliary voltage source. The location of the primary winding produces a variety of topologies by exchanging the primary winding among the terminals of the diagram of Figure 1(a). If the primary winding is connected between terminal '*x*' and '*u*', the voltage at each secondary winding will change according to the main PWM pole commutations, Figure 6(a) for I>0 and Figure 6(b) for I<0.

IV. A CLASS OF MAGNETICALLY COUPLED AUXILIARY POLE FOR ZCZVT INVERTERS

By means of the novel synthesis methodology presented in Section IV, a new family of ZCT and ZCZVT inverters can be disclosed. These inverters are implemented with a Class A AVS, which make them unique. Furthermore, it allows a set of advantages presented only for ZVT inverters hitherto, such as variable timing control for the auxiliary switches and simple design methodology.

The diagram for a novel ZCZVT Class A inverter bridge leg is depicted in Figure 7. This diagram represents the Configuration 1 of Table II. Its main features are the simplicity of the coupled inductor with only two windings and the natural voltage clamp for the auxiliary switches.

A. Principles of Operation

Assuming that load current is flowing in positive direction the ZCZVT inverter with magnetically coupled auxiliary pole assumes twelve different circuit modes in one switching period, as shown in the theoretical waveforms shown in Figure 8. It can be seen that the auxiliary circuit exhibits a linear like current that grows up when auxiliary inductor L_a is magnetized, deviating the main circuit current and also a linear like current when the demagnetization takes place. The resonant intervals are restricted to the charge and discharge of snubber capacitor C_s.

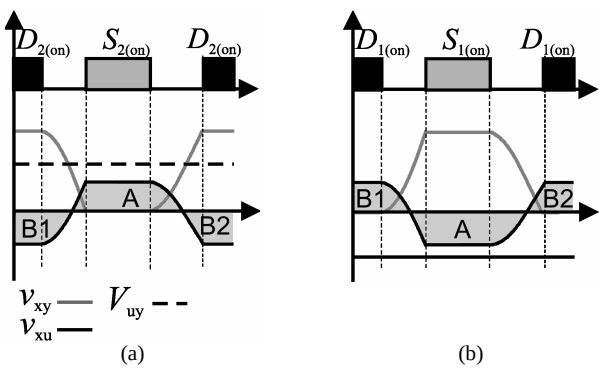

Fig. 6. Waveforms for the primary winding and v_{xy}. (a) I>0; (b) I<0.

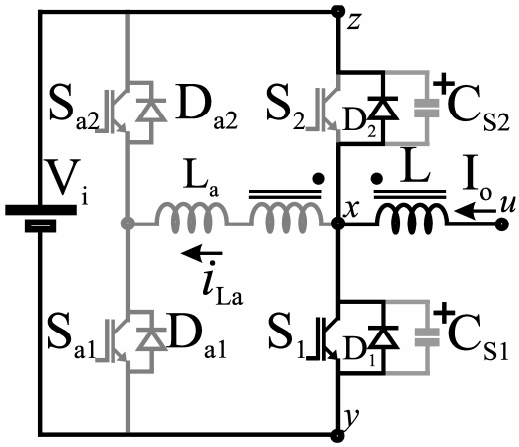

Fig. 7. Novel magnetically coupled auxiliary commutated pole applied to on inverter leg.

The description of each circuit mode for the switch S_1 turn-on process is as follows.

Mode I (t_0,t_1): At instant t_0 the auxiliary switch S_{a1} is turned on and current start to ramp up through auxiliary inductor L_a. Due to the connections of primary and secondary coupled inductor windings, both currents increases. As the secondary winding current rate of rise *di/dt* is larger, current through main diode D_2 decreases proportionally. This mode lasts until current through diode D_2 to be zero. This circuit mode diagram is shown in Figure 9(a).

Mode II (t_1,t_2): When diode D_2 is off, capacitor C_{s1} starts to discharge (C_{s2} discharges) . This resonant process between voltage v_{Cs} and current i_{La} lasts until C_{s1} to be fully discharge. At this instant (t_3) current through both windings reach their

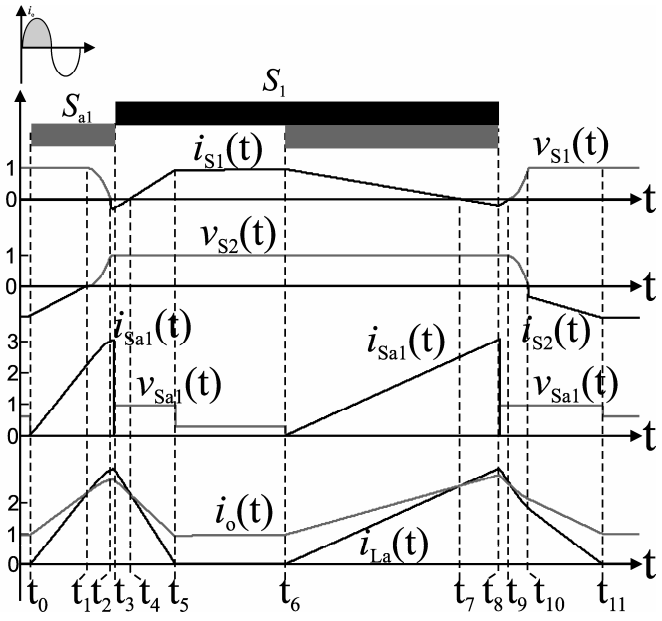

Fig. 8. Theoretical waveforms for the ZCZVT inverter with magnetically coupled auxiliary pole.

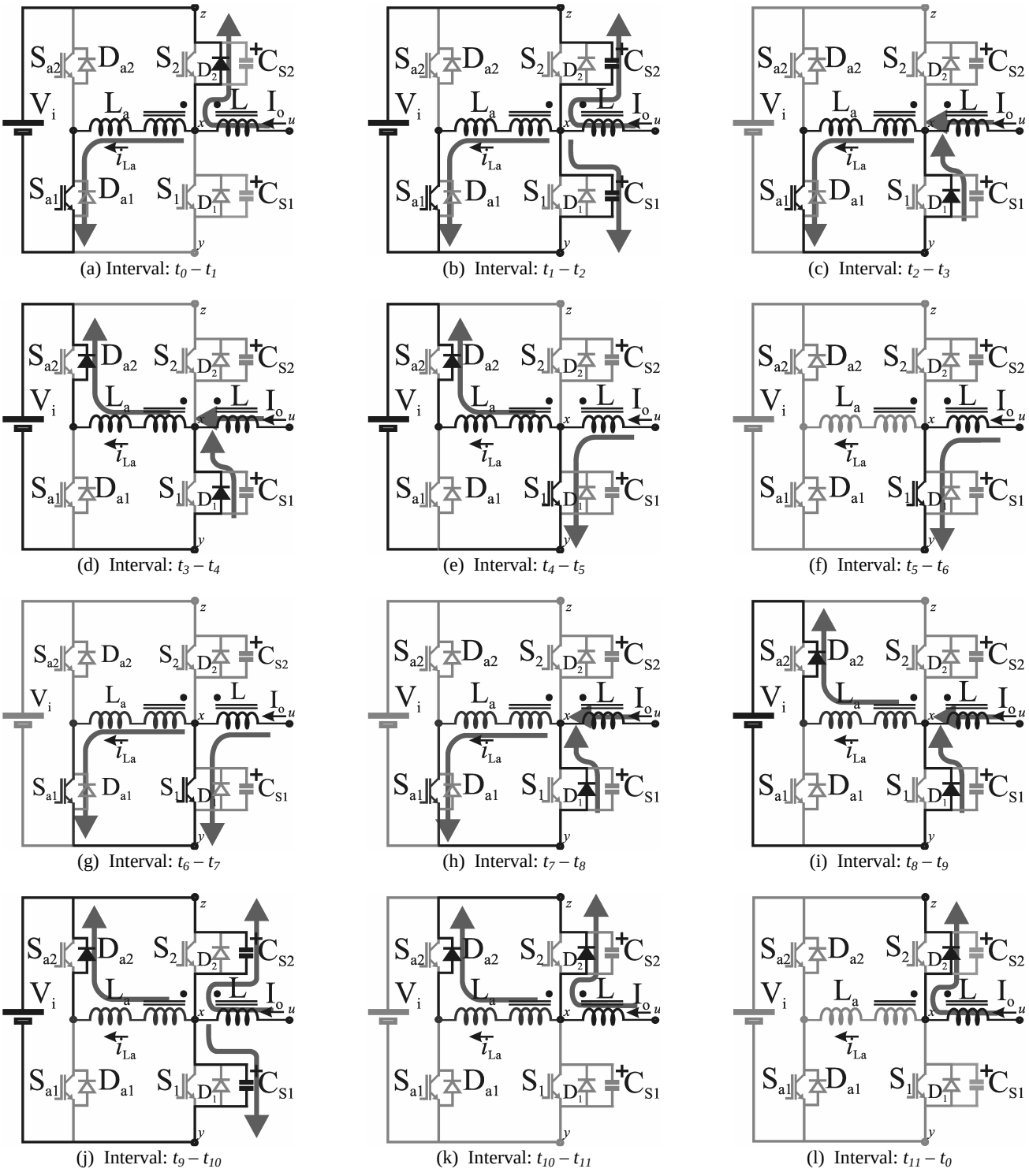

Fig. 9. Circuit mode diagrams for the ZCZVT inverter with magnetically coupled auxiliary pole.

maximum value, as shown in the circuit mode diagram depicted in Figure 9(b).

Mode III (t_2,t_3): When voltage v_{Cs} reaches zero, current through secondary winding is larger than primary winding current, forcing the main diode D_1 starts conducting the difference between these two currents. This situation enables Zero-Current and Zero-Voltage switching conditions to S_1. As voltage across inductor L_a still positive, current i_{La} remains growing. This interval must last until main switch S_1 be driven into the on state. This circuit mode diagram is shown in Figure 9(c).

Mode IV (t_3,t_4): When S_1 is fully turned on, auxiliary switch S_{a1} is turned off in order to demagnetize the auxiliary inductor L_a. At this instant, auxiliary diode D_{a2} turns on. It can be seen that current through primary and secondary windings decreases at different rate of fall (*di/dt*). Until secondary winding current is larger than primary, main diode D_1 conducts their difference. This circuit mode lasts until current to be zero. This circuit mode diagram is shown in

Figure 9(d).

Mode V (t_4,t_5): At instant t_4 primary winding current is larger than the secondary winding current, hence main switch S_1 starts conduct the current difference between these currents. This mode lasts until secondary winding current reaches zero and switch S_1 assume all load current, as can be seen in Figure 9(e).

Mode VI (t_5,t_6): At instant t_5 current through the auxiliary circuit is zero and the inverter operates likewise its hard-switched counterpart , as shown in Figure 9(f). This PWM mode lasts until the main switch S_1 turn-off process starts.

The description of each circuit mode for the switch S_1 turn-off process is as follows.

Mode VII (t_6,t_7): At instant t_6 the auxiliary switch S_{a1} is turned on and current start to rise up through auxiliary inductor L_a in a linear fashion. Once again primary and secondary winding increases with different rate of rises, which diverted the current from switch S_1 to the auxiliary circuit. This mode lasts until primary and secondary winding currents to be equal. At this instant current through main switch S_1 become zero, as can be seen in the circuit diagram shown in Figure 9(g).

Mode VIII (t_7,t_8): Once current through secondary winding is larger than primary winding current, at instant t_7 diode D_1 is turned on conducting the difference between these two currents. This circuit mode enables Zero-Current and Zero-Voltage switching conditions to switch S_1. As voltage across inductor L_a (secondary winding) still positive, current i_{La} remains growing. This interval must lasts until main switch S_1 to be driven off completely. At instant t_8, primary and secondary winding currents reach their second maximum value. This circuit mode diagram is shown in Figure 9(h).

Mode IX (t_8,t_9): Similarly with *Mode IV*, when S_1 is fully turned off, the auxiliary switch S_{a1} is turned off. At this instant, auxiliary diode D_{a2} turns on and auxiliary inductor L_a demagnetizing starts. This mode lasts until main diode D_1 current to be zero and its circuit mode is shown in Figure 9(i).

Mode X (t_9,t_{10}): When diode D_1 is off, capacitor C_{s1} starts to charge-up in a resonant way. This resonant process between voltage v_{Cs} and current i_{La} lasts until C_{s1} to be fully charge at bus voltage V_i. This circuit mode diagram is shown in Figure 9(j).

Mode XI (t_{10},t_{11}): When voltage v_{Cs} reaches V_i, current i_{La} decreases linearly until it become zero. The diagram of this circuit mode can be seen in Figure 9(k).

Mode XII (t_{11},t_{12}): At instant t_{11} current through the auxiliary circuit is zero and the inverter operates likewise its hard-switched counterpart. This PWM mode lasts until the main switch S_1 turn-on process starts. This circuit mode diagram is shown in Figure 9(l).

B. Minimum Voltage and Current Stresses

Differently of the ZCT inverters [5], [16] and the ZCZVT [7,8], it can be seen by means of Figure 8 that voltage and current of the main switches in the ZCZVT inverters with magnetically coupled auxiliary pole are essentially square-waves. As main semiconductor devices are subjected to no additional stresses, they can be rated as the hard-switched counterpart. Similarly, the auxiliary switches are rated for the bus voltage as well as main switches. On the other hand, they operate in a small time interval that is proportional to the load current, thus the auxiliary switch current rating is quite small compared to the main switches.

C. Limited Voltage and Current Transitions

Both ZCT and ZCZVT techniques presented hitherto relay on resonant currents to commutate the PWM pole semiconductors [5], [7], [16]. In these topologies, to ensure that low *di/dt* is applied in these semiconductor transitions, a long resonant period must be considered to the auxiliary resonant components. This situation yields in an exacerbated circulating energy and an extended operating interval for the auxiliary circuit. In the linear like currents of the auxiliary circuits of proposed inverter the low *di/dt* transitions are handled more effectively, just by choosing the right inductance for L_a, which is magnetized right enough to realize the ZCS conditions of the outgoing PWM pole switch.

V. EXPERIMENTAL RESULTS

In order to verify the theoretical analysis presented hitherto, a laboratory prototype of a single-phase inverter, as shown in Figure 10, is implemented. The parameters of this prototype are described in Table III. The single-phase inverter synthesizes a $127V_{rms}$ that feeds a 1kW resistive load, as can be seen in Figure 11(a). The main and auxiliary semiconductors are implemented with 2-pack IGBT modules, ensuring the modularity of the set-up. Switches S_1

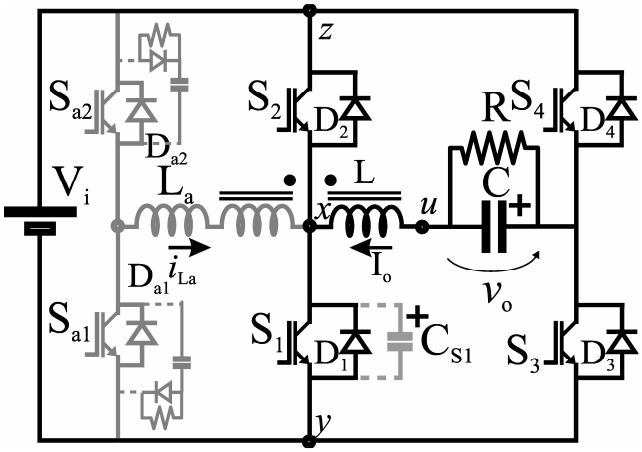

Fig. 10. Diagram of the Novel single-phase H-bridge ZCZVT with magnetically coupled auxiliary pole inverter.

TABLE III
ZCZVT prototype experimental parameters.

Parameter	ZCZVT
V_i / V_0	250 V_{CC} / 127 $V_{(RMS)}$
P_0 / f_s	1,0 kW / 40 kHz
L (L_M) / C *(filter)*	0,93 mH (L_M) / 2 x 20 uF
S_1, S_2, S_3, S_4	SK45GB063
S_{a1}, S_{a2}	SK45GB063
N (n_2/n_1)	0,42 (18 turns/45 turns)
L_{k1} , L_{k2} *(leakages)*	24,9 µH / 4,7 µH
L_a *(aux. inductor)*	4,7 µH (L_{k2})
C_S *(aux. capacitor)**	4,7 nF
$R_{Sn1,2}$ / $C_{Sn1,2}$ / $D_{Sn1,2}$	100 Ω / 4,3 nF / UF5406
Spike killer	SA 14x8x4.5 (8 turns)

* In the ZCT prototype C_s=0.

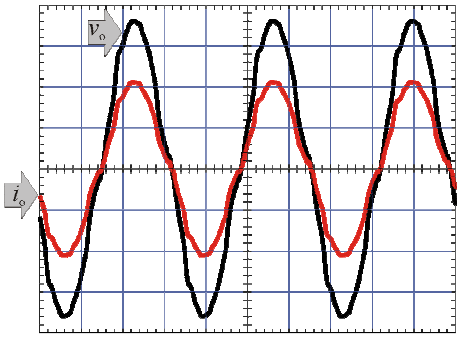

(a) Scales: i_o – 5A/div; v_o – 50V/div; time - 5ms/div.

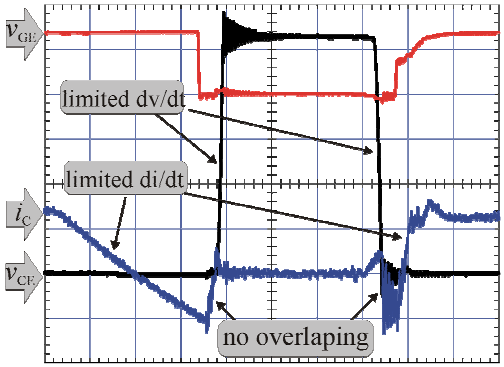

(b) Scales: v_{GE} – 10V/div; i_C – 5A/div ; v_{CE} – 50V/div; time – 2us/div.

Fig. 11. Experimental waveforms of the single-phase ZCZVT with magnetically coupled auxiliary pole inverter prototype.

and S_2 commutate at 40 kHz and are assisted by the auxiliary switches S_{a1} and S_{a2}, respectively. The zero voltage and current conditions for S_1 can be observed in Figure 11(b). It can be seen that both, *di/dt* and *dv/dt* across the main device is limited during the switching intervals. The coupled inductor is implemented with a two windings Ferrite EE-69/33/52 core. As the current through the outgoing diode is always zero before commutations the value of the snubber capacitor C_s is only defined by the maximum allowable *dv/dt* of the main switches. For the IGBT, the snubber capacitor C_s can be made as smaller as possible, in order to reduce the ringing of its voltage and current probe parasitic inductance.

Figure 12 shows comparative waveforms for the main switching turn-on and turn-off waveforms for a 4.7 nF and a zero C_s capacitance. It is ease to see that main switch dv/dt is much higher with no parallel capacitor, in both, turn-on Figure 12(a) and turn-off Figure 12(c). Nevertheless, a current lower frequency resonance is more perceived in the presence of C_s, as can be seen for the turn-on Figure 12(b) and turn-off Figure 12(d). These characteristics will be decisive in the EMI performance of the inverter.

The auxiliary switching S_{a1} waveforms are analyzed in Figure 13. In spite of a short current spike due to the discharge of its turn-off RCD snubber, the current through S_{a1} presents a linear like form, ensuring low reactive energy during the turn-on process of main switch S_1 Figure 13(a). Similarly, Figure 13(b) shows the auxiliary switch S_{a1} waveforms during the turn-off process of S_1. It can be seen that the current rises up linearly until the switch turns off. The discharge of the turn-off RCD snubber during this process is almost meaningless, once right after S_1 had

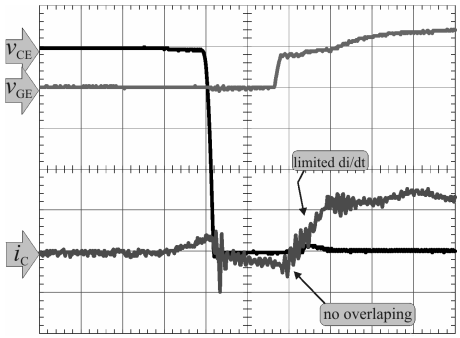

(a) w.o. Cs

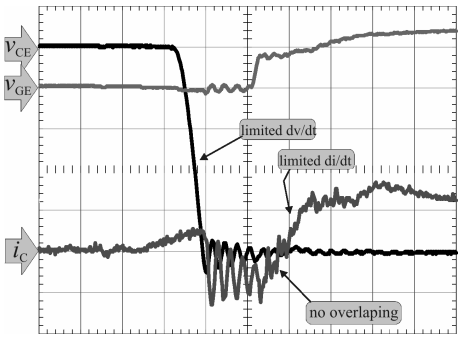

(b) w. Cs

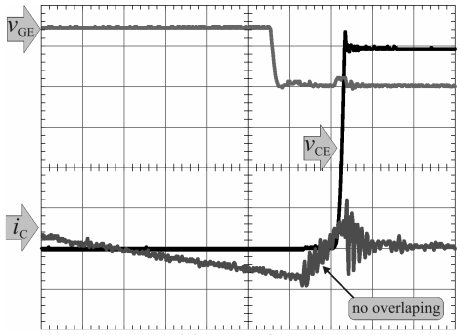

(c) w.o. Cs

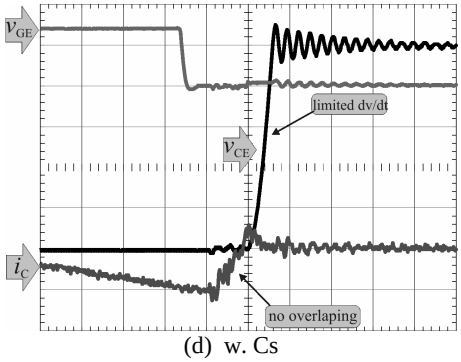

(d) w. Cs

Scales: v_{GE} – 10V/div; i_o – 5A/div; v_o – 50V/div; time – 500ns/div.

Fig. 12. Experimental waveforms of the single-phase ZCZVT with magnetically coupled auxiliary pole inverter prototype.

assumed the load current, almost whole energy stored in the auxiliary turn-off snubber to be regenerated to the load through S_1.

In order to access the gains of the proposed ZCZVT inverter an experimental comparative analysis of a set of laboratory prototypes was carried out. For this analysis, the DC bus voltage has been implemented with a three phase bridge rectifier and a step down transformer, producing a

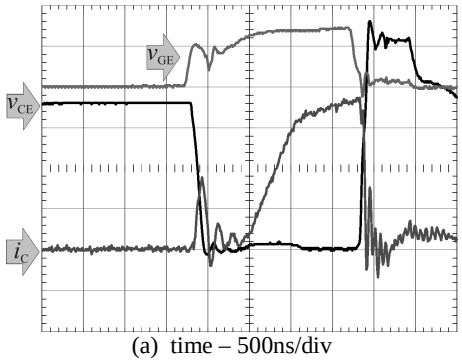

(a) time – 500ns/div

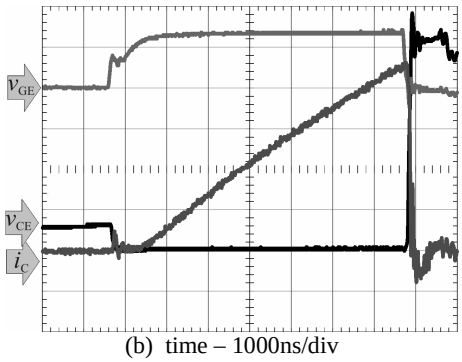

(b) time – 1000ns/div

Scales: v_{GE} – 10V/div; i_o – 5A/div; v_o – 50V/div.

Fig. 13. Experimental waveforms of the single-phase ZCZVT with magnetically coupled auxiliary pole inverter prototype.

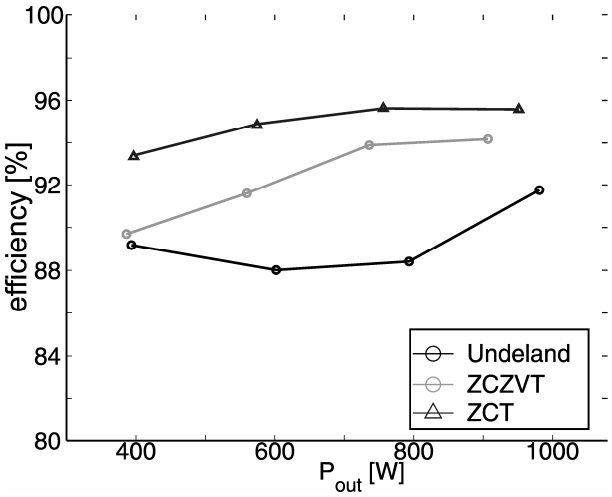

Fig. 14. Experimental efficiency curves.

360V DC voltage. The efficiency curves are shown in Figure 14 for three different prototypes. The ZCZVT inverter was compared to a dissipative Undeland snubber inverter and a ZCT inverter (C_s=0). The choice of using the snubber of Undeland is twofold, first it is more efficient than an ordinary RCD snubber and it can represent the operation of the Inverter without the ZCZVT auxiliary circuit since the hard switched prototype was not feasible at the power and frequency specifications. On the other hand, the ZCT prototype has been chosen in order to evaluate its impact on the efficiency. It can be seen that the ZCZVT and ZCT prototypes presented better efficiency than that of the Undeland prototype for the entire load range, mainly due to the slightly lower auxiliary current stress. The ZCZVT prototype achieved 94.2% of efficiency at full load and the ZCT prototype presented a slight high efficiency, achieving 95.5% at full load. The prototype of the Undeland inverter presented the lowest efficiency among all experimental prototypes, which proves that the ZCZVT inverter with magnetically coupled auxiliary pole is a strong candidate to replace the hard-switched and conventional ZCT and ZCZVT inverters.

VI. CONCLUSIONS

This paper presented a simple, novel and unique methodology to analyze the Resonant Transition technique mechanism. It presents a qualitative analysis which is carried out based on the auxiliary voltage source (AVS) concept. Employing this concept to the resonant transition turn-on (ZVT technique) and turn-off (ZCT technique) the requirements of the resonant transition mechanism (zero-voltage and zero-current) are identified, allowing an easy way to perceive their main characteristics and limitations. The qualitative analysis split the Resonant Transition converters into two main classes of converters in function of AVS: (i) the *continuous time varying* AVS and (ii) the *discontinuous* AVS resonant transition converters. As demonstrated in the paper, the resonant transition analysis can be used as a synthesis methodology of novel converters. Furthermore, the qualitative analysis reveals that there is an opportunity to generate two entire classes of converters, the *Class A ZCT* and the *Class A ZCZVT* converters. The *Class A* (*discontinuous* AVS) permit to the ZCT and ZCZVT converters hold features only presented by ZVT converters before, such as variable timing control, low reactive energy, simple control, etc..

To illustrate the usefulness of the proposed Resonant Transition Concept, which analysis reveals that there is an opportunity to generate a entire family of converters, based on the *Class A* AVS, the Novel ZCZVT inverters with non-resonant auxiliary circuit are derived. The *Class A* AVS permit to the ZCZVT inverters hold features only presented by ZVT inverters before, such as variable timing control, low reactive energy, simple control, and so on.

Theoretical analysis is verified by means of experimental results obtained from laboratory prototypes rated at 1kW, 40kHz. The results proved the feasibility of the novel inverters, allowing the main semiconductors to operate with Zero-Current and Zero-Voltage switching conditions. Furthermore, the auxiliary switches present a linear like current shape, which amplitude varies proportionally with the load current. It also must be paid attention that an adequate design of the auxiliary components should be important to the EMI performance of the prototype.

ACKNOWLEDGEMENT

The authors would like to express their gratitude to "Coordenação de Aperfeiçoamento de Pessoal de Nível Superior – CAPES" and "Conselho Nacional de Desenvolvimento Científico e Tecnológico – CNPQ" (proc. nº 311096/2006-9 and nº 481195/2007-6) for financial support.

REFERENCES

[1] N.A. Moguilnaia, *et al*, "Innovation in Power Semiconductor Industry: Past and Future", *IEEE Transactions on Engineering Management*, vol. 52, n° 4, pp. 429-439, November 2005.

[2] V.K. Khana, *The Insulated Gate Bipolar Transistor IGBT: Theory and Design*, IEEE Press, Piscataway, NJ, 2003.

[3] G. Majumdar, "Power Modules As Key Component Group For Power Electronics", *in Proc. of the Power Conversion Conference -. PCC '07*, pp. P-1 – P-8, 2007.

[4] R.L. Steigerwald, "Power electronic converter technology" *in Proc. of the IEEE*, vol. 89, n°. 6, June 2001, pp. 890-897.

[5] Y. Li, F.C. Lee, D. Boroyevich, "A Three-Phase Soft-Transition Inverter with a Novel Control Strategy for Zero-Current and Near Zero-Voltage Switching", *IEEE Transactions on Power Electronics*, vol. 16, n°. 5, pp. 710-723, September 2001.

[6] C.A. Canesin, I. Barbi, "Estudo Experimental Comparativo das Perdas entre Seis Diferentes Conversores do Tipo Boost com 1.6kw, usando I GBTs", *Eletrônica de Potência* - SOBRAEP, vol. 1, n°. 1, pp. 26-34, 1996.

[7] C.M.O. Stein, *et al*, "Zero-Current and Zero-Voltage Soft-Transition Commutation Cell for PWM Inverters", *IEEE Transactions on Power Electronics*, vol. 19, no. 2, pp. 396-403, 2004.

[8] C.M.O. Stein, H.L. Hey, "Conversor Boost ZCZVT PWM", *Eletrônica de Potência* - SOBRAEP, vol. 3, n°, 1 pp. 35-41, 1998.

[9] X. Jing, D. Boroyevich, "Comparison between a novel zero-switching-loss topology and two existing zero-current-transition topologies", *in Proc. of IEEE Applied Power Electronics Conference* APEC '00, vol. 2, pp. 1044-1048, 2000.

[10] J.L. Russi, M.L. Martins, H.L. Hey, "Zero-Voltage Transition PWM Converters: a Classification Methodology", *IEE Electric Power Application*, vol. 152, n°. 2, pp. 323-334, March 2005.

[11] J. Dawidziuk, S. Jalbrzykowski, Z. Prajs, "A Comparative Analysis and Experimental Studies of Resonant Commutated Pole Inverter", *in IEEE Proc. of IECON*, pp. 328-332, 1994.

[12] Y. Li, F.C. Lee, D. Boroyevich, "A Simplified Three-Phase Zero- Current-Transition Inverter with Three Auxiliary Switches", *IEEE Transactions on Power Electronics*, vol. 18, no. 3, pp. 802-813, May 2003.

[13] Y. Li, F.C. Lee, D. Boroyevich, "A Simplified Three-Phase Zero-Current-Transition Inverter with Three Auxiliary Switches", *IEEE Transactions on Power Electronics*, vol. 18, n°. 3, pp. 802-813, May 2003.

[14] M.L. Martins, J.L. Russi, H. L. Hey, "Novel Synthesis Methodology for Resonant Transition PWM Converters", *in Proc. of COBEP*, 2005.

[15] M.L. Martins, J.L. Russi, J.R. Pinheiro, H.L. Hey, "Zero-current Zero-voltage Transition PWM Converters With Magnetically Coupled Auxiliary Circuit", *Eletrônica de Potência* - SOBRAEP, vol 13, n°. 4, pp. 201-208, 2008.

[16] M. Hengchun, *et al*, "Improved zero-current transition converters for high-power applications", *IEEE Transactions on Industry Applications*, vol. 33, n°. 5, pp.1220-1232, September/October, 1997.

BIOGRAPHIES

Mário Lúcio da Silva Martins was born in Palmeira das Missões, RS, Brazil, in 1976. He received the B.S. (1999), M.S. (2002) and Ph.D. (2008) degrees in electrical engineering from the Federal University of Santa Maria. In 2006, he joined the Department of Electronics of the Federal Technological University of Parana where he is currently a Professor. Dr. Martins is a member of the Brazilian Power Electronics Society (SOBRAEP).

Carlos Marcelo de O. Stein was born in Santiago, RS, Brazil, in 1970. He received the B.S. (1996), M.S. (1997) and Ph.D. (2003) degrees in electrical engineering from the Federal University of Santa Maria, Santa Maria, Brazil. Since 2003, he has been with the UTFPR, Pato Branco, Parana, Brazil, where he is currently a Professor. His research interests include high-frequency power converter topologies, power-factor-correction techniques, power supplies, and soft-switching techniques. Dr. Stein is a member of the Brazilian Power Electronics Society (SOBRAEP).

Jumar L. Russi was born in Passo Fundo, Brazil, in 1977. He received the B.S., (2000) M.S. (2003) and the Ph.D. (2007) degrees from the Federal University of Santa Maria, Santa Maria, Brazil in electrical engineering. From 1998 to 2007, he has been with the Power Electronics and Control Research Group (GEPOC), Federal University of Santa Maria. In 2007 he joined the Federal University of Pampa where he is actually a professor. His research interests include switched-mode power supplies, uninterruptible power supplies, and high-performance power converters.

José Renes Pinheiro was born in Santa Maria, Brazil, in 1958. He received the B.S. (1981) degree from the Federal University of Santa Maria, Santa Maria, Brazil, and the M.S. (1984) and Ph.D. (1994) degrees from the Federal University of Santa Catarina, Florianópolis, Brazil, all in electrical engineering. Since 1985, he has been a Professor at the Federal University of Santa Maria. From 2001 to 2002, he was with the Center for Power Electronics Systems, Virginia Polytechnic Institute and State University, Blacksburg, as a Postdoctoral Research Scholar. Dr. Pinheiro is a member of the Brazilian Power Electronics Society, Brazilian Automatic Control Society, and several IEEE societies.

Hélio Leães Hey was born in Santa Maria, Brazil, in 1961. He received the B.S. (1985) degree from the Catholic University of Pelotas, Pelotas, Brazil, and the M.S. (1987) and Ph.D. (1991) degrees from the Federal University of Santa Catarina, Florianopolis, Brazil. From 1989 to 1993, he was with the Federal University of Uberlândia, Uberlândia, Brazil. Since 1994, he has been with the Power Electronics and Control Research Group (GEPOC), Federal University of SantaMaria, where he is currently a Professor. From 1995 to 1999, he was Editor of the Brazilian Power Electronics Journal. Dr. Hey is a member of the Brazilian Power Electronics Society, Brazilian Automatic Control Society, and several IEEE societies.